Journal of Advanced Research in Numerical Heat Transfer

Journal homepage:
https://semarakilmu.com.my/journals/index.php/arnht/index
ISSN: 2735-0142

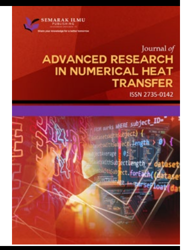

Influence of Substrate Tilting Angle on Graphene Production Through Atmospheric Pressure Chemical Vapor Deposition

Syed Noh Syed Abu Bakar[1,*], Muhammad Naqib Osman[1], Mohd Azan Mohammed Sapardi[1], Mohd Hanafi Ani[2], Mohd Firdaus Abd Wahab[3], Yose Fachmi Buys[4]

[1] Department of Mechanical and Aerospace Engineering, Kulliyyah of Engineering, International Islamic University Malaysia, Jalan Gombak, 53100 Kuala Lumpur, Malaysia
[2] Department of Manufacturing and Materials Engineering, Kulliyyah of Engineering, International Islamic University Malaysia, Jalan Gombak, 53100 Kuala Lumpur, Malaysia
[3] Department of Chemical Engineering and Sustainability, Kulliyyah of Engineering, International Islamic University Malaysia, Jalan Gombak, 53100 Kuala Lumpur, Malaysia
[4] Department of Mechanical Engineering, Faculty of Industrial Technology, Universitas Pertamina, Indonesia

ARTICLE INFO

Article history:
Received 25 August 2024
Received in revised form 26 September 2024
Accepted 23 October 2024
Available online 30 November 2024

ABSTRACT

Chemical Vapor Deposition (CVD) is a promising method for producing graphene. However, the reaction environment, such as the flow field inside the CVD reactor, remains poorly understood. Therefore, the current study focused on the influence of the substrate tilting angle on the graphene quality and elucidating the flow field around the substrate. An experiment using atmospheric pressure chemical vapor deposition (APCVD) and a simulation study of substrate tilting angle in graphene production are presented. The graphene is produced using APCVD for 8°, 15°, and 60° substrate tilting angles. The Raman characterization was done on all the substrates to see the effect of the substrate tilting angle on the graphene produced. A computational fluid dynamics (CFD) model of the heating chamber of the CVD chamber was developed using ANSYS® FLUENT to understand the result further. Simulation for the three titling angles was performed using the developed CFD model. The experimental results showed that the best result was graphene produced by tilting an angle at 15° while the lowest quality was at a 60° tilting angle. This indicates an optimum tilting angle at a lower tilting angle. The simulation revealed the relationship between vorticity and boundary layer thickness to the graphene quality.

Keywords:
Graphene; Tilting angle; Boundary layer; Vorticity; APCVD

1. Introduction

The discovery of graphene in 2004 sparked immense interest among researchers due to its exceptional properties, including structural and fracture strength [1], thermal and electrical conductivity [2], and flexibility. These characteristics have positioned graphene as a promising material for various applications, such as optoelectronics, flexible solar cells, bio-sensing, nanocomposites, and energy storage devices [3-5]. While mechanical exfoliation, the method used

* *Corresponding author.*
E-mail address: syednoh@iium.edu.my (Syed Noh Syed Abu Bakar)

https://doi.org/10.37934/arnht.27.1.2844

by Novoselov *et al.*, [6] in their first graphene discovery in 2004, can produce high-quality graphene, it is limited to small-scale production. Chemical vapor deposition (CVD), which utilizes carbon-containing precursor gas mixed with carrier gases to deposit graphene on a metal substrate, is the most promising method for producing scalable, large-area, high-quality graphene films [7-9]. However, the complex phenomena involved in the CVD process require careful attention to control the quality of the graphene produced.

The synthesis of graphene via CVD is influenced by several factors that interact in complex ways, affecting various aspects of graphene growth, such as uniformity, growth speed, and morphology [10]. These factors include pressure inside the growth chamber, heating temperature, substrate material, and the type of precursor gas and its mixture with carrier gases. The pressure inside the growth chamber can be atmospheric [11,12], low-pressure [13-16], high-pressure [17] or ultra-high vacuum [18]. On the other hand, the heating temperature for APCVD is typically around 900 °C to 1000 °C [22-27], although attempts have been made to synthesize graphene at lower temperatures (< 800 °C) [28-34]. Substrate materials, such as copper [31;32,36-38], nickel [26,27,35,36], ruthenium [41,42], cobalt [43,44], platinum [41], and iridium [42], play a crucial role in catalyzing the reaction, with copper being the most reported substrate. The choice of precursor gas (e.g., [28,43], acetylene [26,27,44], methane [36,49-51], and benzene [29] and its mixture with carrier gases (e.g., Argon, hydrogen, or oxygen) also significantly influences the quality of synthesized graphene [12]. Changing the mixture composition affects the chemical reaction inside the chamber and alters the flow behavior of the gas mixture, which in turn impacts the quality of the graphene produced.

In addition to these factors, the thermal-fluidic aspect has been recognized as crucial in CVD film deposition since the 1970s, although it has not gained as much attention in graphene production by CVD. Researchers have included flow behavior in mathematical models for epitaxial silicon growth [48], demonstrated the importance of coupling flow equations with species concentration equations in modeling LPCVD for single-wafer reactors [49], and shown that both fluid dynamics and chemical kinetics significantly influence the growth rate [50]. Flow visualization experiments have highlighted issues such as return flows at the leading edge of heated susceptors in cold-wall CVD [51]. In contrast, the entrance effect on gas flow patterns and temperature profiles in epitaxial systems using various gas carriers has been emphasized [56,57]. Numerical models coupling fluid dynamics and chemical kinetics have demonstrated the critical effect of gas velocity on gas concentration profiles and deposition rates [54]. More recently, the importance of thermal-fluidic aspects in graphene deposition using hot-wall APCVD has been shown [14, 28, 42], and a critical review has examined the influence of fluid dynamics on graphene systems via APCVD, considering the range of Reynolds numbers used in graphene deposition and their impact on graphene quality [12]. Osman *et al.*, [57] have highlighted the importance of substrate placement in avoiding developing and recirculation regions.

The substrate tilting angle is a critical aspect of substrate geometry that significantly influences the synthesis of uniform deposits in CVD processes. Researchers have investigated the effects of tilting angles on deposition uniformity since the 1970s. Eversteyn *et al.*, [48] predicted that a small substrate tilting angle would produce better uniformity along the substrate. Bulsari *et al.*, [58] studied convective heat and mass transfer in a horizontal CVD reactor with a tilted susceptor, concluding that an inclined susceptor tends to provide a more uniform deposition away from the leading edge. Fotiadis *et al.*, [59] found that tilting the susceptor from 0° to 18.4° provides more uniform temperature gradients, leading to more uniform deposition. Khanafer and Lightstone [60] further demonstrated that a tilted susceptor can produce more significant deposition and uniform distribution than a non-tilted susceptor. However, they noted a maximum angle beyond which the tilting angle no longer positively contributes to deposition quality. Cheng and Hsiao [61] have shown

that tilting the substrate effectively suppresses the return flow size and strength, influencing deposition uniformity.

The uniformity of the boundary layer is another essential factor in graphene growth, and it is closely related to the substrate tilting angle. Although return flow is not an issue for hot wall CVD, other flow characteristics, such as the boundary layer thickness influenced by substrate tilting angle, may play a role in growth uniformity. Zhang *et al.*, [62] discussed that placing the substrate parallel to the flow will introduce a nonuniform (hydrodynamic) boundary layer compared to the tilted substrate. Bhaviripudi *et al.*, [63] discussed that at high synthesis temperatures (> 900 °C), growth in APCVD is limited (thus governed) by diffusion through the boundary layer. At the same time, the reaction on the substrate surface limits growth in LP or UHV. Li *et al.*, [56] reported similar findings and arguments. In a review paper, Lui *et al.*, [64] provided a subsection reviewing the study of the boundary layer in CVD, but none of the reviewed studies expressly referred to graphene production. The substrate tilting angle significantly influences the uniformity of the boundary layer in CVD processes, which in turn affects the uniformity and quality of graphene growth, particularly in APCVD at high synthesis temperatures. Further research is needed to understand better the relationship between substrate tilting angle, boundary layer characteristics, and graphene growth to improve the ability to control the quality of graphene synthesized via CVD. By optimizing the substrate tilting angle and boundary layer uniformity, researchers may enhance the uniformity and quality of graphene films produced using CVD methods, paving the way for more advanced applications of this remarkable material.

The tilting angle is one of the essential factors in synthesizing uniform deposition via CVD. However, to the authors' knowledge, very few have studied this factor for graphene deposition. Understanding the influence of this factor may improve the ability to control the quality of graphene synthesis via CVD. Therefore, the current paper focuses on elucidating the gas flow behavior when the substrate tilting angle and its relation to the quality of graphene is produced. The graphene is synthesized using CVD for 8°, 15°, and 60° substrate tilting angles. The Raman characterization was done on all the substrates to see the effect of the substrate tilting angle on the graphene produced. To further understand the result, the heating chamber of the CVD chamber was modeled by using ANSYS® FLUENT. Simulation for several titling angles was performed using the model. The CFD result was analyzed to understand the effect of the substrate tilting angle on the bulk flow and boundary layer thickness. Finally, the graph of monolayer ratio and defect ratio against boundary layer thickness was plotted to see the effect of boundary layer thickness on the graphene produced.

2. Methodology

In the present work, to determine the influence of the substrate tilting angle on the quality of graphene synthesized, a series of experimental works was performed to synthesize graphene on the copper substrate via atmospheric pressure CVD for several substrate tilting angles. The grown graphene quality for each tilting angle was inspected using Raman spectroscopy. Three spots on the substrate were taken for Raman characterization for each tilting angle—the graphitic peaks of D, G, and 2D show the presence of graphene. The D-peak is the structural defects such as disorders at the plane, grain boundaries, and domain edges [9]. The G-peak corresponds to the center vibration of carbon atoms and is a standard feature for graphene and carbon graphitic materials [65]. A 2D peak is used to determine the number of graphene layers. The I_D, I_G, and I2D represent the intensity of the D, G, and 2D peaks. Their ratios will be used to indicate the graphene quality. The ratio of I_{2D}/I_G indicates a graphene layer which is single-layer, bilayer, and few layers of graphene when $I_{2D}/I_G > 2$,

$1 < I_{2D}/I_G < 2$, and $I_{2D}/I_G < 1$, respectively. Meanwhile, a smaller defect ratio of I_D/I_G indicates better graphene quality.

The reaction environment inside the CVD reactor remains poorly understood. A computational method, such as computational fluid dynamics (CFD), can help identify the measurable external parameters that control the reaction environment [67]. Many studies have utilized CFD to study flow dynamics, heat transfer, and species transport [69,71,73,75,77]. In the current study, a CFD model was developed to elucidate further the influence of substrate tilting angles on the grown graphene quality. The flow characteristics, such as streamlines, vorticity, and boundary layers around the substrate, were analyzed.

2.1 Experimental Method

The copper substrate was polished and cleaned thoroughly using an ultrasonic sonicator. It was then cut to a standard size of 1×1 cm^2. The substrate was then placed on an 8° holder and put inside the CVD tube with a diameter of 1.5 cm and length of 100 cm. There was a 28 cm heated section along this tube where the copper substrate was placed, as shown in Figure 1.

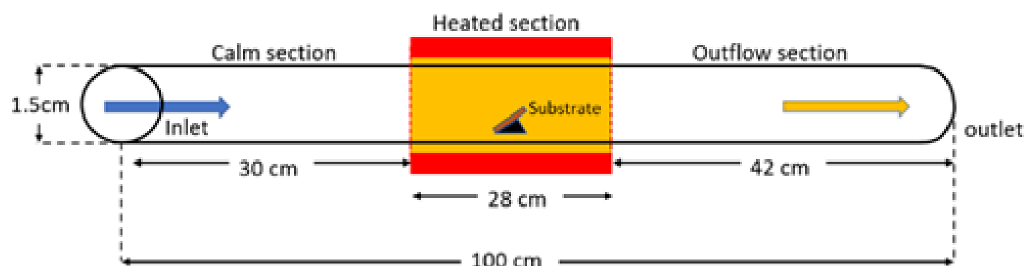

Fig. 1. Schematics of the CVD tube

The tube was sealed and purged before Argon was supplied to the tube, and the heat was provided at the heated section. After 20 minutes, once the temperature inside the heated section reached 1273 K, hydrogen gas was supplied to the flow to start the annealing process for 20 minutes. After that, methane was provided to the flow for 5 minutes for graphene growth. The total flow rate during the growth is 300 sccm (282 sccm of Argon, 15 sccm for hydrogen and 3 sccm for methane). After that, the substrate was left to cool to room temperature in an argon environment [59]. This whole process is depicted in Figure 2. The process was repeated for substrate tilting angles of 15° and 60°.

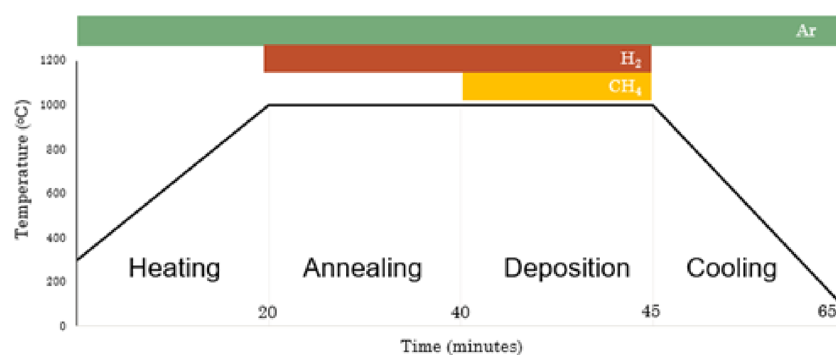

Fig. 2. Gas use for each process during the synthesis process

2.2 Characterization

Raman spectroscopy was used to characterize the deposited samples. The samples were characterized directly on the substrates without transfer. The intensity of the Raman peak was extracted from the maximum value after baseline subtraction over the corresponding spectral range (1300 cm^{-1} to 1400 cm^{-1} for the D peak, 1560 cm-1 to 1600 cm-1 for the G peak, and 2620 cm-1 to 2760 cm-1 for the 2D peak). For each substrate, three different spots were taken for Raman characterization: the leading edge, the middle, and the end of the substrate, as shown in Figure 3. All these three spots were along the centreline of the substrate (along the C-line). The results from the Raman Characterization were analyzed. The monolayer and defect ratios were calculated to observe the substrate tilting angle's influence on the synthesized graphene's quality.

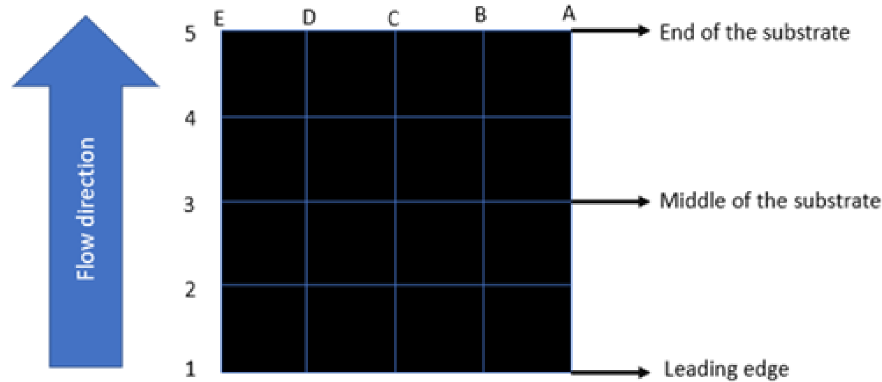

Fig. 3. The Coordinates of the line on the substrate and the location of Raman characterization were taken.

2.3 Numerical Method

To elucidate the flow characteristic inside the heated chamber, particularly around the substrate, a 3D CFD model was developed using ANSYS® Fluent. The model is a simplified model without incorporating chemical reactions. Since argon gas is the bulk composition of the gas mixture (94% of the gas mixture is Argon), it is assumed that the argon gas will dictate the flow behavior. Therefore, only Argon is used in this model.

2.3.1 Physical descriptions and boundary conditions

The schematic drawing of the model is depicted in Figure 1, and the boundary conditions setup is summarized in Figure 4. The tube wall material was set to quartz, and the substrate material was set to copper. A uniform temperature (isothermal) of 1273 K was imposed on the tube wall within the heated section, and 300 K was imposed at the calm and outflow section. The substrate was set to adiabatic. Velocity at all solid surfaces was set to no-slip condition. The gas used was set to an incompressible ideal gas. This incompressible ideal gas condition in ANSYS® Fluent implies that the density may change due to the temperature change but remains constant with pressure. This allows the model to capture any buoyancy effects that may influence the gas flow upon entering the heated region. The inlet was set to a constant velocity of 0.0283 m/s, corresponding to a flow rate of 300 sccm. The Reynolds number was calculated based on the tube diameter and inlet velocity, which gave a value of 25.15. Based on Cengel *et al.*, [60], internal flow with a Reynolds number less than 2000 for a circular tube is categorized as laminar flow. The outlet was set to outflow, and the calculated

parameters' gradients were set to zero. The substrate was modeled without its holder. Three substrate tilting angles were used, which were 8°, 15°, and 60°. Although Fauzi *et al.*, [55] showed that a simulation with or without gravitational acceleration did not show many different results in terms of flow behavior close to the substrate, in the current model, the gravitational acceleration of 9.81 m/s^2 in the negative y-direction (downward) was applied to emulate the gravitational effect.

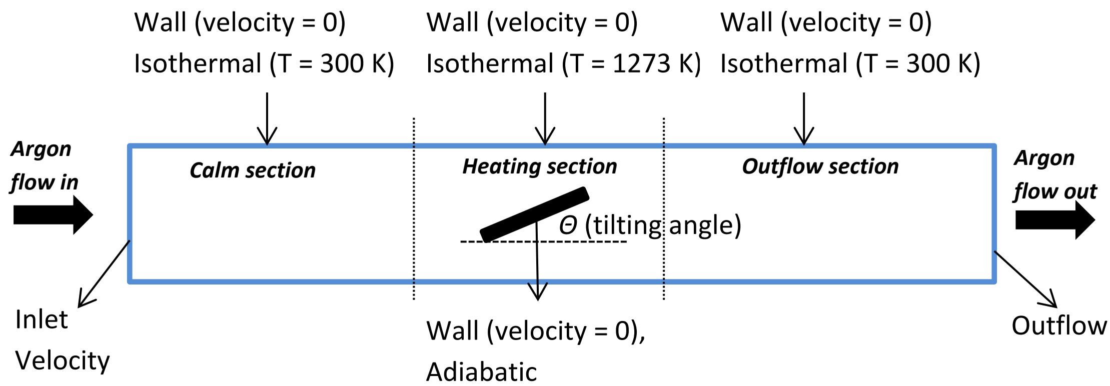

Fig. 4. Boundary conditions set up

2.3.2 Simulation setup

Since the calculated Reynolds number for the current model shows that the flow is laminar, a laminar model is used. The grid at the heated region is smaller than at the other section, as in Figure 5, where the orange line represents the furnace's inlet. Then, a face meshing technique was used at the wall so that the grid size was the same in every section. For the whole 3D model, there are 7.7 million mesh elements.

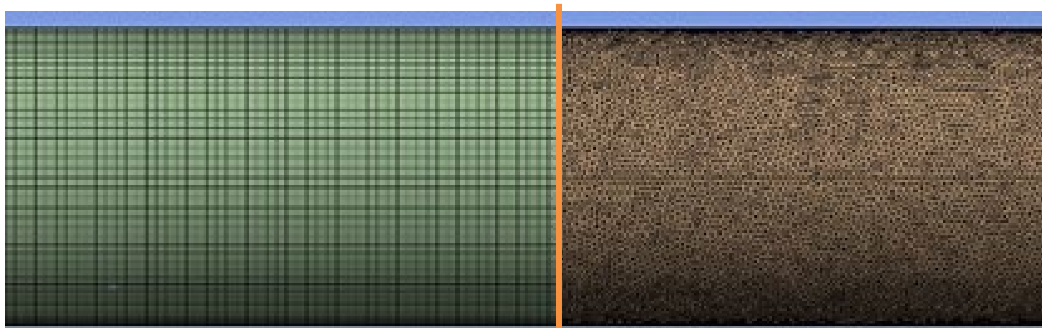

Fig. 5. The mesh different from the non-heated section to the heated section

The operating pressure is set to standard atmospheric pressure, thus representing APCVD. Table 1 shows the details of the setup.

Table 1
The setup used for the CFD simulation

Solver type		Pressure Based
Gravitational Acceleration		9.81 m/s^2
Time		Steady
Model		Laminar
Solution method	Scheme	SIMPLEC
	Pressure	PRESTO!
	Momentum	Second-Order Upwind
	Energy	Second-Order Upwind
Gauss-Seidel iterative methods		Residuals < 1 × 10^{-6}

2.3.4 Hydrodynamic boundary layer

Once the simulation was completed, the flow behavior for each tilting angle was analyzed, and the boundary layer thickness was obtained. There are three types of boundary layers: the hydrodynamics boundary layer, the thermal boundary layer, and the mass boundary layer. All three boundary layers refer to the behavior of each transport property: momentum, thermal energy, and mass. In analyzing each boundary layer, velocity variation indicates the hydrodynamics boundary layer, temperature variation is used for the thermal boundary layer, and species concentration is used for the mass boundary layer. This article discusses only the hydrodynamic boundary layer, which will be called the boundary layer for simplicity. The hydrodynamic boundary layer is a region where the viscous effect is significant. For an internal flow where solid walls bind fluid flow, the thickness of the boundary layer is bounded by this wall and lies somewhere between the two walls. For fully developed flows inside a straight, circular tube, such as the bulk flow far away from the substrate, the boundary layer is the radius of the tube.

The boundary layer thickness is determined from the wall until the maximum velocity location along a line perpendicular to the surface. Once the flow is disrupted by a particular obstruction, the substrate, in the current case, the boundary layer, is altered, and now the thickness lies somewhere between the tube wall and the substrate. Since this study is interested in studying the boundary layer thickness over the substrate, the boundary layer is calculated from the substrate surface to the maximum velocity magnitude along the perpendicular line. There are 25 lines perpendicular to the substrate, as shown in Figure 6. Boundary layer thickness across the plate for each tilting angle will be presented. The behavior of the boundary layer thickness on the plate will be analyzed and related to the graphene produced for each tilting angle.

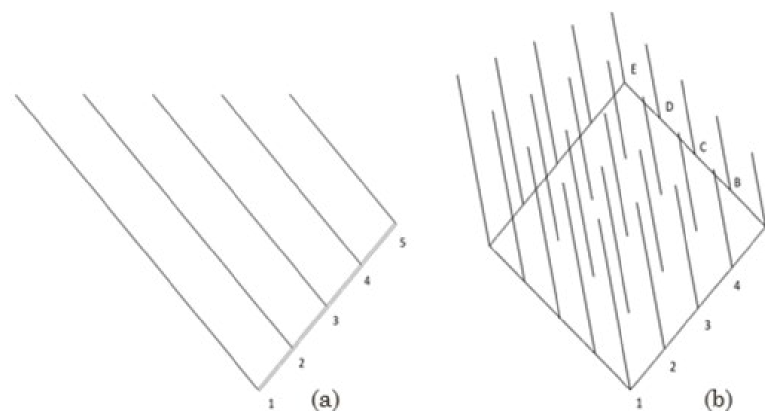

Fig. 6. Line used to obtain the boundary layer at each point. (a) The side view of the substrate (b) The overview of the substrate

2.4 CFD Model Validation

The validation case is based on a study by McComas and Eckert [66], where the Grashof number is 492 and the Reynolds number is 743. Figure 7 shows the schematic model of the tube used for the validation. The tube has a diameter D of 0.0127 m. The tube is divided into two sections, the unheated and heated sections. The unheated section has a length of L_c, which is 0.25 m. This section is for the flow to develop before fully entering the unheated section. The unheated section has a length of L_h, which is 0.889 m. The wall of the unheated section (along L_c) is set as an insulated wall (zero heat flux), while a constant heat flux of 83.46 W/m^2 was supplied directly at the tube wall of the heated section (along L_h).

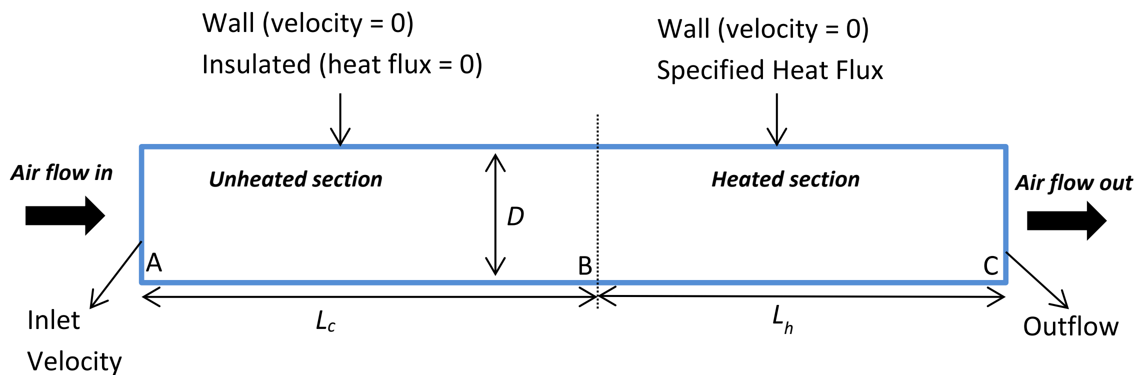

Fig. 7. Schematic drawing of the CFD validation model and boundary condition setup

The fluid used for this validation case is air. The operating pressure was set as 30.80 kPa, which gives air density and viscosity of 0.467 kg/m^3 and 1.493 kg/m·s, respectively. A line was drawn along the top wall to get the temperature along the top wall. Five cross-sectional planes were drawn along the tube to determine the bulk temperature. The data obtained from the simulation was plotted and compared with the data from the experimental work of McComas and Eckert [66]. As shown in Figure 8, the results agreed with the experimental work, and the highest calculated error was 0.34 % only.

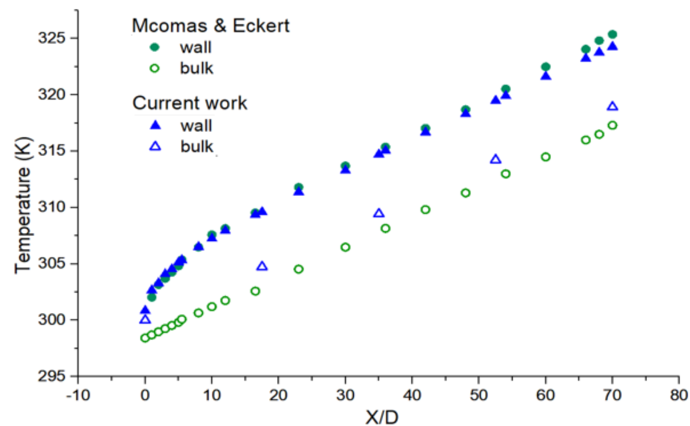

Fig. 8. Graph of the wall and bulk temperature against X/D with the filled symbol representing wall temperature and hollow symbol for bulk temperature

2.5 Scope and Limitation

The CVD processes for producing graphene involve several methods, such as heating, annealing, growing, and cooling for specific periods and various mixtures of gases. However, for simplicity, this CFD study only examines the growing period. The flow is considered to be steady. In addition, the chemical reaction is also excluded from this study, thus focusing only on the thermal-fluidic phenomena in CVD without the complexity of the chemical reaction. Since Argon dominates the composition of the mixture during the growth period, only Argon is used in this CFD analysis. The CFD study made here is simply an attempt to elucidate the macroscopic behavior of the gas flow within the reaction chamber, mainly flow over the substrate surface.

3. Results and Discussions

3.1 Results of Raman Spectroscopy for Various Tilting Angles

Figure 9 shows the I_D/I_G and I_{2D}/I_G ratio on the three spots along the centerline for each tilting angle. The I_D/I_G ratio provides insights into the defect density within the graphene layers for different substrate tilting angles. At an 8° tilt, the I_D/I_G ratio increases from the front to the end. This trend suggests an increase in defects towards the end of the substrate. For the 15° tilt, the I_D/I_G ratio remains low, slightly increasing at the end. This indicates minimal defect formation. In contrast, the 60° tilt shows a significant increase in the I_D/I_G ratio from the front to the end, highlighting a substantial rise in defects. Therefore, it can be said that Lower tilting angles produced better graphene since it produced fewer layers and fewer defects.

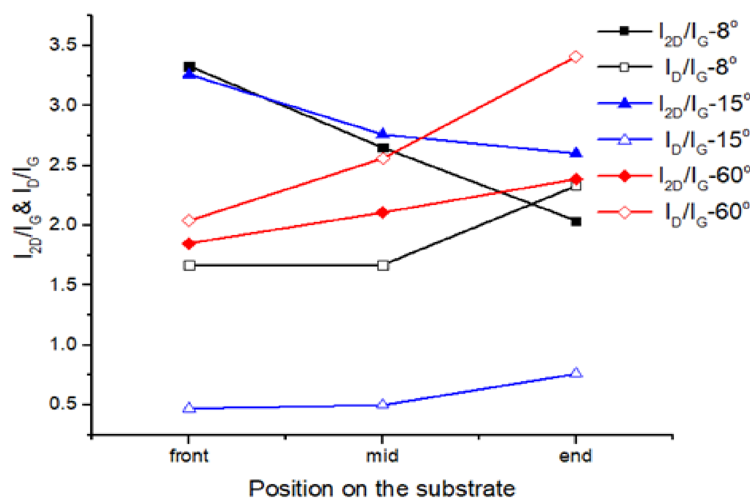

Fig. 9. Monolayer and defect ratio from the Raman spectroscopy result

The I_{2D}/I_G ratio reflects the number of graphene layers and their quality. For the 8° tilt, the ratio decreases from the front to the end, indicating a reduction in graphene quality or increased layer thickness towards the end. At a 15° tilt, the I_{2D}/I_G ratio is relatively stable, decreasing from the front to the end. Conversely, the 60° tilt shows an increase in the I_{2D}/I_G ratio from the front to the end. This variability indicates inconsistent graphene quality.

Overall, the results show that while the defect increases, the number of layers decreases from the front edge to the end edge of the substrate. Furthermore, examining the ratios for all three tilting angles, one may see that the tilting angle of 15° produced the best quality graphene regarding the

number of layers and defects. This suggests an optimum tilting angle, which lies somewhere at the lower tilting angle, in producing high-quality graphene.

3.2 Flow Behavior Around Substrate for Different Tilting Angles

Examining flow character around the substrate using CFD results reveals two things that may explain the influence of the tilting angles on the graphene quality. As shown in Figure 10, the gas flows faster at the substrate's end edge than at the front edge. This is indicated by the denser streamline as well as the color contour. The 8° and 15° tilting angles exhibit similar characteristics of flow, where the streamlines are relatively uniform and parallel, with the 15° tilt showing a gradual increase in velocity. A more noticeable characteristic of 60° tilting angles is the appearance of a stagnation point on the substrate, which divides the flow into two regions. One region flows over the top while the other flows through the bottom. The flow near the splitting region shows a slow-flowing gas. This indicates that the flow over higher tilting angles may involve more complex flow dynamics. This results in more consistent graphene quality, as indicated by the relatively stable I_D/I_G and I_{2D}/I_G ratios from front to end. The results in Figure 9 show that the number of graphene layers is higher towards the back end of the substrate except for the 60° tilting angle. This coincides with the region where the flow is faster. The number of layers for the 8° tilting angle shows a continuously increasing pattern. In contrast, for the 15° tilting angle, the number of layers somewhat remains similar towards the back end of the substrate. As reported by several researchers, such as Li et al. [68], the graphene quality produced decreased along the flow direction due to the depletion of carbon sources as the gas flows.

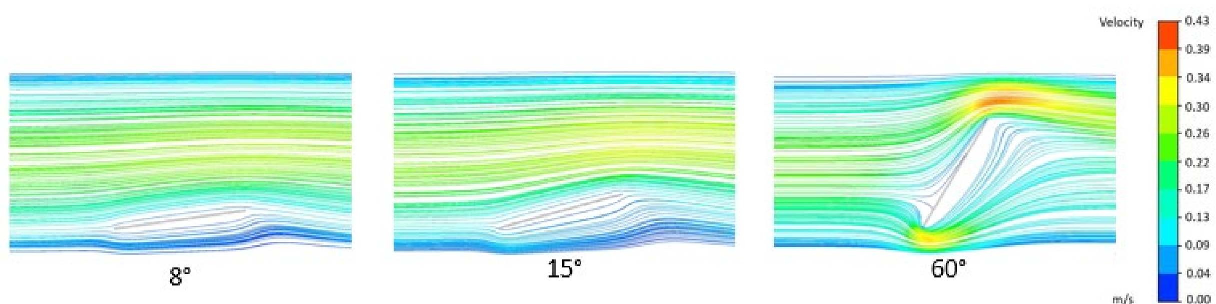

Fig. 10. Streamline near the substrate along the centerline.

Secondly, as seen in Figure 10, the flow velocity gradient is steeper towards the end of the substrate—the steeper velocity gradient results in higher vorticity. Vorticity is best described as the degree of fluid particle rotation. Fluid particles may rotate as they flow as an object rotating as it moves along its orbit. The steep velocity gradient and high vorticity also indicate high shear stress. Figure 11 shows the vorticity contour along the substrate. The vorticity distribution is more uniform for 8° and 15° tilting angles, except there is a slight increase towards the end of the 15° tilting angle.

On the other hand, the vorticity distribution is not uniform across the surface of the 60° angle substrate. In addition to the nonuniform vorticity, high vorticity existence can be seen clearly in the 60° angle substrate. This indicates a more predictable and calm flow over the lower tilting angles, while the flow is more complex for substrates with high tilting angles.

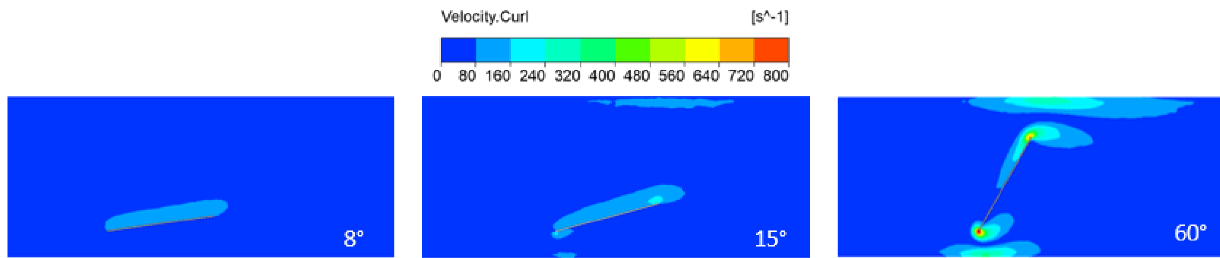

Fig. 11. Vorticity contours the centreline of the substrate.

3.3 Hydrodynamic Boundary Layer

In this study, the boundary layer thickness is indicated by the perpendicular distance from the substrate to the location of the maximum velocity. The distance is measured along a straight line, as shown in Figure 6. Figure 6 also indicates the 25 locations where the boundary thickness is determined. The determined boundary layer thickness for each location is shown in Figure 12. The result clearly shows that the higher the substrate angle, the lesser the uniformity of the boundary layer is. The behavior of the fluid velocity over the substrate may explain this observation. As the angle of the substrate increases, the cross-sectional area for the fluid to pass through becomes smaller. Therefore, this forces the fluids near the substrate's edge to move faster than flow near the substrate's middle. The higher the angle, the faster fluid flow at the edge. This behavior is confirmed by the streamline shown in Figure 10. The color contour (yellow to red indicate higher velocity) and the streamline density (denser streamline indicates higher velocity) suggest that the velocity is higher at the edge for the 60° tilted substrate than the 8° tilted substrate.

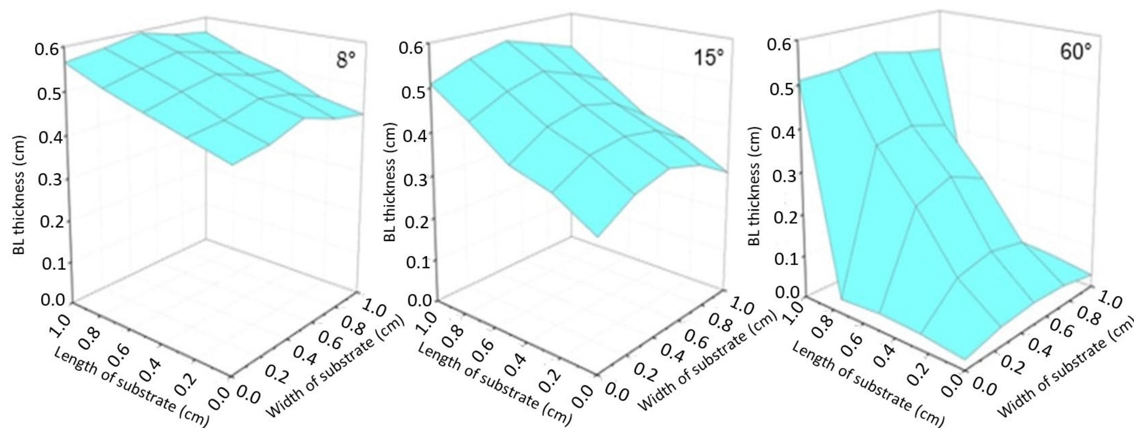

Fig. 12. Boundary layer (BL) thickness over the substrate

Most discussions involving CVD boundary layers have focused on the boundary layer thickness variation along the flow direction. However, Figure 12 reveals the boundary layer distributed across the substrate surface area. The boundary layer thickness is almost homogeneous across the surface for a slight tilting angle, such as 8° and 16° tilting angles, except there is a slight decrease for 16° tilting angles. At a higher tilting angle, such as in the case of 60°, the boundary layer thickness is dramatically changed along the flow direction and in the direction perpendicular to the flow direction. Although Raman spectroscopy results in Figure 9 reveal only the graphene quality variation along the flow direction, it is believed that a similar trend of graphene quality to boundary layer thickness can be seen if one studies the graphene quality across the width of the substrate.

3.4 Relating Flow Behavior to the Quality of the Graphene

The results showed that while a complex flow around the substrate is not desired since it produces low-quality graphene, a calm and predictable flow does not necessarily produce better-quality graphene. Therefore, this suggests an optimum tilting angle for producing high-quality graphene.

A flow with complex phenomena, such as steep changes in flow velocity, vorticity, and boundary layer thickness, not only contributes to the non-uniformity of the graphene growth but also leads to high defects. In particular, one can see a direct correlation between vorticity distribution and the defect of the graphene produced. The defect tends to be higher at high vorticity regions. Mizuno & Uekusa [70-71] and Mizuno et al. [74] also reported a correlation between the deposition quality and the vorticity distribution across a substrate. In particular, Mizuno & Uekusa [72] have shown that the qualitative behavior of the vorticity distribution is similar to that of the deposition rate over the substrate.

In the graphene growth mechanism, methane gas, as the carbon source for the growth, needs to be sufficiently transported to the substrate surface, and the by-product must be removed from the surface. In this regard, vorticity helps enhance mass transport by mixing the region of low methane concentrations at the substrate surface after the nucleation with higher concentrations away from the surface. However, Figure 9 and Figure 11 results indicate that excessive vorticity leads to nonuniform graphene growth and high defects.

Vorticity is generated by shear stress due to the velocity gradient. When there is a velocity gradient between fluid layers, shear stresses are created, which induce the rotation of fluid elements, thus creating vorticity. Excessive vorticity indicates excessive shear stress on the substrate surface, which may increase dislocation density, contribute to void formation, or induce stress-related defects such as stacking faults and twin boundaries. The relationship between shear stress and defect formation is often material-specific and depends on the particular growth conditions. Shear stress also significantly influences nucleation. Higher shear stress usually promotes the increase of the nucleation density, leading to more rapid initial film coverage and finer grain structures. This can be advantageous for applications requiring uniform, fine-grained films. However, for processes where large, high-quality thin films are desired, such as graphene, lower shear stress conditions might be preferable to allow for slower, more controlled nucleation and growth.

The results of Figures 9 to 12 confirmed that high tilting angles result in steep changes in flow behavior, such as streamline pattern, vorticity distribution, and boundary layer thickness—these result in nonuniform and high graphene defects. However, a significantly low tilting angle, such as an 8° tilt, produces gradual changes in flow behavior and better-quality graphene; the defects are still high (but lower when compared to a 60° tilt). This can be explained by comparing the vorticity distribution and boundary layer thickness for 8° and 16° tilt. The vorticity is slightly higher, and the boundary layer thickness is lower with a more gradual change at a 16° tilt. Both factors enhanced mass transport to the surface: higher vorticity enhances mixing, and lower boundary layer thickness makes the precursor easier to diffuse from the gas phase to the surface. Fauzi *et al.*, [55] have shown that the monolayer ratio correlates well with boundary thickness. They reported that the thinner the boundary layer, the higher the monolayer ratio (indicating higher quality graphene). Stock and Richter [76] stated that the higher the flow rate for a cold reactor, the thinner the boundary layer will be. They argued that this, in turn, will lead to a narrower high-temperature zone closer to their susceptor, which will lead to a more homogeneous deposition.

Generally, optimal deposition conditions are achieved when the flow field is carefully controlled to balance various factors. Better deposition typically occurs when vorticity and boundary layer

thickness enhance mass transfer and promote uniform nucleation without causing excessive turbulence or stress-induced defects. This often requires fine-tuning reactor design, such as substrate tilting angle. Conversely, poor deposition can result from insufficient shear stress and a thick boundary layer (which leads to mass transfer limitations and nonuniform growth) or excessive shear stress (causing turbulence, high defect densities, or nonuniform nucleation).

4. Conclusions

Gas flow behavior when the substrate tilting angle and its relation to the quality of graphene produced are elucidated in the current study. The synthesized graphene quality for 8°, 15°, and 60° substrate tilting angles has been studied. The Raman characterization revealed the effect of the substrate tilting angle on the graphene produced. The results showed that, among the tested angles, the tilting angle of 15° produced the best quality of graphene. Based on the graphene quality and tilting angle trends, it can be concluded that there is an optimum tilting angle for producing quality graphene. Furthermore, the tilting angle, such as 15° and below, must be lower.

To further understand the result, the heating chamber of the CVD chamber was modeled by using ANSYS® FLUENT. Simulation for several titling angles was performed using the model. The simulation results revealed two critical parameters that can be linked to graphene quality: vorticity and boundary layer thickness. The results showed that high vorticity and non-uniformity of vorticity distribution contributed to a lower quality of graphene (higher defects across the substrate surface). With many other findings indicating that a better quality of graphene is produced at higher flow velocity, a compromise between vorticity and velocity required further study. This is because flow at higher velocity usually will lead to higher vorticity and shear stress close to a solid surface.

Analysis of boundary layer thickness agreed with many other studies, which showed that the thinner the boundary layer, the better quality graphene. Tilting the substrate angle may result in a thinner boundary layer at the edge of the substrate. However, tilting at a high angle created a highly nonuniform boundary layer. It also showed the importance of paying attention to the boundary layer thickness distribution over the whole area of the substrate. The results showed that the boundary layer thickness changes not only in the direction of the bulk flow but also in the direction perpendicular to the bulk flow.

The current study has been limited to a steady, single-phase flow without gas reaction to elucidate the flow field in CVD using CFD. Future CFD work should include gas reaction in the chamber and the time factor (since graphene growth is limited to a period). In addition, this study's characterization of graphene quality has been limited to Raman spectroscopy readings on three points along a line. More comprehensive readings may give further insights into the influence of the flow field on graphene quality.

Acknowledgment

This work was financially supported by the Fundamental Research Grant Scheme (FRGS/1/2019/TK03/UIAM/02/5 or FRGS19-145-0754) and the Ministry of Higher Education Malaysia (MOHE).

References

[1] Lee, Changgu, Xiaoding Wei, Jeffrey W. Kysar, and James Hone. "Measurement of the elastic properties and intrinsic strength of monolayer graphene." *science* 321, no. 5887 (2008): 385-388. https://doi.org/10.1126/science.1157996

[2] Mayorov, Alexander S., Roman V. Gorbachev, Sergey V. Morozov, Liam Britnell, Rashid Jalil, Leonid A. Ponomarenko, Peter Blake et al. "Micrometer-scale ballistic transport in encapsulated graphene at room temperature." *Nano letters* 11, no. 6 (2011): 2396-2399. https://doi.org/10.1021/nl200758b

[3] Azam, Mohd Asyadi, Nor Najihah Zulkapli, Norasimah Dorah, Raja Noor Amalina Raja Seman, Mohd Hanafi Ani, Mohd Shukri Sirat, Edhuan Ismail, Fatin Bazilah Fauzi, Mohd Ambri Mohamed, and Burhanuddin Yeop Majlis. "Critical considerations of high quality graphene synthesized by plasma-enhanced chemical vapor deposition for electronic and energy storage devices." *ECS Journal of Solid State Science and Technology* 6, no. 6 (2017): M3035. https://doi.org/10.1149/2.0031706jss

[4] Mishra, Neeraj, John Boeckl, Nunzio Motta, and Francesca Iacopi. "Graphene growth on silicon carbide: A review." *physica status solidi (a)* 213, no. 9 (2016): 2277-2289. https://doi.org/10.1002/pssa.201600091

[5] Ani, M. H., M. A. Kamarudin, A. H. Ramlan, E. Ismail, M. S. Sirat, M. A. Mohamed, and M. A. Azam. "A critical review on the contributions of chemical and physical factors toward the nucleation and growth of large-area graphene." *Journal of materials science* 53 (2018): 7095-7111. https://doi.org/10.1007/s10853-018-1994-0

[6] Novoselov, Kostya S., Andre K. Geim, Sergei V. Morozov, De-eng Jiang, Yanshui Zhang, Sergey V. Dubonos, Irina V. Grigorieva, and Alexandr A. Firsov. "Electric field effect in atomically thin carbon films." *science* 306, no. 5696 (2004): 666-669. https://doi.org/10.1126/science.1102896

[7] Zhang, Y. I., Luyao Zhang, and Chongwu Zhou. "Review of chemical vapor deposition of graphene and related applications." *Accounts of chemical research* 46, no. 10 (2013): 2329-2339. https://doi.org/10.1021/ar300203n

[8] Vlassiouk, Ivan, Sergei Smirnov, Murari Regmi, Sumedh P. Surwade, Nishtha Srivastava, Randall Feenstra, Gyula Eres et al. "Graphene nucleation density on copper: fundamental role of background pressure." *The Journal of Physical Chemistry C* 117, no. 37 (2013): 18919-18926. https://doi.org/10.1021/jp4047648

[9] Zhang, Jia, PingAn Hu, Xiaona Wang, Zhenlong Wang, Danqin Liu, Bin Yang, and Wenwu Cao. "CVD growth of large area and uniform graphene on tilted copper foil for high performance flexible transparent conductive film." *Journal of Materials Chemistry* 22, no. 35 (2012): 18283-18290. https://doi.org/10.1039/c2jm33881e

[10] Zhang, Yi, Luyao Zhang, Pyojae Kim, Mingyuan Ge, Zhen Li, and Chongwu Zhou. "Vapor trapping growth of single-crystalline graphene flowers: synthesis, morphology, and electronic properties." *Nano letters* 12, no. 6 (2012): 2810-2816. https://doi.org/10.1021/nl300039a

[11] Vlassiouk, Ivan, Pasquale Fulvio, Harry Meyer, Nick Lavrik, Sheng Dai, Panos Datskos, and Sergei Smirnov. "Large scale atmospheric pressure chemical vapor deposition of graphene." *Carbon* 54 (2013): 58-67. https://doi.org/10.1016/j.carbon.2012.11.003

[12] Fauzi, Fatin Bazilah, Edhuan Ismail, Mohd Hanafi Ani, Syed Noh Syed Abu Bakar, Mohd Ambri Mohamed, Burhanuddin Yeop Majlis, Muhamad Faiz Md Din, and Mohd Asyadi Azam Mohd Abid. "A critical review of the effects of fluid dynamics on graphene growth in atmospheric pressure chemical vapor deposition." *Journal of Materials Research* 33, no. 9 (2018): 1088-1108. https://doi.org/10.1557/jmr.2018.39

[13] Gürsoy, Mehmet, Emre Çıtak, and Mustafa Karaman. "Uniform deposition of large-area graphene films on copper using low-pressure chemical vapor deposition technique." *Carbon Letters* 32, no. 3 (2022): 781-787. https://doi.org/10.1007/s42823-021-00309-3

[14] Lee, Byoungdo, Weishen Chu, and Wei Li. "Effects of process parameters on graphene growth via low-pressure chemical vapor deposition." *Journal of Micro-and Nano-Manufacturing* 8, no. 3 (2020): 031005. https://doi.org/10.1115/1.4048494

[15] Yang, Meng, Shinichirou Sasaki, Ken Suzuki, and Hideo Miura. "Control of the nucleation and quality of graphene grown by low-pressure chemical vapor deposition with acetylene." *Applied Surface Science* 366 (2016): 219-226. https://doi.org/10.1016/j.apsusc.2016.01.089

[16] Borah, Munu, Abhishek K. Pathak, Dilip K. Singh, Prabir Pal, and Sanjay R. Dhakate. "Role of limited hydrogen and flow interval on the growth of single crystal to continuous graphene by low-pressure chemical vapor deposition." *Nanotechnology* 28, no. 7 (2017): 075602. https://doi.org/10.1088/1361-6528/aa527e

[17] Yousefian, Pedram, and Siddha Pimputkar. "Computational fluid dynamics modeling of a new high-pressure chemical vapor deposition reactor design." *Journal of Crystal Growth* 566 (2021): 126155. https://doi.org/10.1016/j.jcrysgro.2021.126155

[18] Mueller, Niclas S., Anthony J. Morfa, Daniel Abou-Ras, Valerio Oddone, Tymoteusz Ciuk, and Michael Giersig. "Growing graphene on polycrystalline copper foils by ultra-high vacuum chemical vapor deposition." *Carbon* 78 (2014): 347-355. https://doi.org/10.1016/j.carbon.2014.07.011

[19] Deng, Bing, Zhaowei Xin, Ruiwen Xue, Shishu Zhang, Xiaozhi Xu, Jing Gao, Jilin Tang et al. "Scalable and ultrafast epitaxial growth of single-crystal graphene wafers for electrically tunable liquid-crystal microlens arrays." *Science Bulletin* 64, no. 10 (2019): 659-668. https://doi.org/10.1016/j.scib.2019.04.030

[20] Cho, Joon Hyong, Jason J. Gorman, Seung Ryul Na, and Michael Cullinan. "Growth of monolayer graphene on nanoscale copper-nickel alloy thin films." *Carbon* 115 (2017): 441-448. https://doi.org/10.1016/j.carbon.2017.01.023

[21] Wang, Ziwen, Zhongying Xue, Miao Zhang, Yongqiang Wang, Xiaoming Xie, Paul K. Chu, Peng Zhou, Zengfeng Di, and Xi Wang. "Germanium-assisted direct growth of graphene on arbitrary dielectric substrates for heating devices." *Small* 13, no. 28 (2017): 1700929. https://doi.org/10.1002/smll.201700929

[22] Deng, Bing, Zhenqian Pang, Shulin Chen, Xin Li, Caixia Meng, Jiayu Li, Mengxi Liu et al. "Wrinkle-free single-crystal graphene wafer grown on strain-engineered substrates." *ACS nano* 11, no. 12 (2017): 12337-12345. https://doi.org/10.1021/acsnano.7b06196

[23] Zakar, Eugene, A. Glen Birdwell, Kevin Hauri, Richard X. Fu, Cheng Tan, and Madan Dubey. "Controlling defects in fine-grained sputtered nickel catalyst for graphene growth." *Journal of Vacuum Science & Technology B* 36, no. 2 (2018). https://doi.org/10.1116/1.4998441

[24] Lavin-Lopez, M. P., J. L. Valverde, S. Ordoñez-Lozoya, A. Paton-Carrero, and A. Romero. "Role of inert gas in the Cvd-graphene synthesis over polycrystalline nickel foils." *Materials Chemistry and Physics* 222 (2019): 173-180. https://doi.org/10.1016/j.matchemphys.2018.09.083

[25] Yoon, Hahnjoo, Dong Su Shin, Taek Gon Kim, Dohyun Kim, and Jinsub Park. "Facile synthesis of graphene on Cu nanowires via low-temperature thermal CVD for the transparent conductive electrode." *ACS Sustainable Chemistry & Engineering* 6, no. 11 (2018): 13888-13896. https://doi.org/10.1021/acssuschemeng.8b02135

[26] Martin, M-B., B. Dlubak, R. S. Weatherup, M. Piquemal-Banci, Heejun Yang, Raoul Blume, Robert Schlögl et al. "Protecting nickel with graphene spin-filtering membranes: A single layer is enough." *Applied Physics Letters* 107, no. 1 (2015). https://doi.org/10.1063/1.4923401

[27] Weatherup, Robert S., Bruno Dlubak, and Stephan Hofmann. "Kinetic control of catalytic CVD for high-quality graphene at low temperatures." *ACS nano* 6, no. 11 (2012): 9996-10003. https://doi.org/10.1021/nn303674g

[28] Sun, Xiao, Li Lin, Luzhao Sun, Jincan Zhang, Dingran Rui, Jiayu Li, Mingzhan Wang et al. "Low-temperature and rapid growth of large single-crystalline graphene with ethane." *Small* 14, no. 3 (2018): 1702916. https://doi.org/10.1002/smll.201702916

[29] Jang, Jisu, Myungwoo Son, Sunki Chung, Kihyeun Kim, Chunhum Cho, Byoung Hun Lee, and Moon-Ho Ham. "Low-temperature-grown continuous graphene films from benzene by chemical vapor deposition at ambient pressure." *Scientific reports* 5, no. 1 (2015): 17955. https://doi.org/10.1038/srep17955

[30] Zheng, Li, Xinhong Cheng, Peiyi Ye, Lingyan Shen, Qian Wang, Dongliang Zhang, Ziyue Gu, Wen Zhou, Dengpeng Wu, and Yuehui Yu. "Decreasing graphene synthesis temperature by catalytic metal engineering and thermal processing." *RSC advances* 8, no. 3 (2018): 1477-1480. https://doi.org/10.1039/C7RA11654C

[31] Lampert, Lester F., Roman Caudillo, Thomas Lindner, and Jun Jiao. "C-plane sapphire and catalyst confinement enable wafer-scale high-quality graphene growth." *The Journal of Physical Chemistry C* 120, no. 46 (2016): 26498-26507. https://doi.org/10.1021/acs.jpcc.6b06459

[32] Fauzi, Fatin Bazilah, Edhuan Ismail, Muhammad Naqib Osman, Muhammad Suffian Rosli, Ahmad Faris Ismail, Mohd Ambri Mohamed, Syed Noh Syed Abu Bakar, and Mohd Hanafi Ani. "Influence of mixed convection in atmospheric pressure chemical vapor deposition of graphene growth." *Materials today: proceedings* 7 (2019): 638-645. https://doi.org/10.1016/j.matpr.2018.12.055

[33] Kim, Keun Soo, Yue Zhao, Houk Jang, Sang Yoon Lee, Jong Min Kim, Kwang S. Kim, Jong-Hyun Ahn, Philip Kim, Jae-Young Choi, and Byung Hee Hong. "Large-scale pattern growth of graphene films for stretchable transparent electrodes." *nature* 457, no. 7230 (2009): 706-710. https://doi.org/10.1038/nature07719

[34] Li, Xuesong, Weiwei Cai, Jinho An, Seyoung Kim, Junghyo Nah, Dongxing Yang, Richard Piner et al. "Large-area synthesis of high-quality and uniform graphene films on copper foils." *science* 324, no. 5932 (2009): 1312-1314. https://doi.org/10.1126/science.1171245

[35] Reina, Alfonso, Stefan Thiele, Xiaoting Jia, Sreekar Bhaviripudi, Mildred S. Dresselhaus, Juergen A. Schaefer, and Jing Kong. "Growth of large-area single-and bi-layer graphene by controlled carbon precipitation on polycrystalline Ni surfaces." *Nano Research* 2 (2009): 509-516. https://doi.org/10.1007/s12274-009-9059-y

[36] Reina, Alfonso, Xiaoting Jia, John Ho, Daniel Nezich, Hyungbin Son, Vladimir Bulovic, Mildred S. Dresselhaus, and Jing Kong*. "Layer area, few-layer graphene films on arbitrary substrates by chemical vapor deposition." *Nano letters* 9, no. 8 (2009): 3087-3087. https://doi.org/10.1021/nl901829a

[37] Sutter, Peter W., Jan-Ingo Flege, and Eli A. Sutter. "Epitaxial graphene on ruthenium." *Nature materials* 7, no. 5 (2008): 406-411. https://doi.org/10.1038/nmat2166

[38] Yang, K., W. D. Xiao, Y. H. Jiang, H. G. Zhang, L. W. Liu, J. H. Mao, H. T. Zhou, S. X. Du, and H-J. Gao. "Molecule–substrate coupling between metal phthalocyanines and epitaxial graphene grown on Ru (0001) and Pt (111)." *The Journal of Physical Chemistry C* 116, no. 26 (2012): 14052-14056. https://doi.org/10.1021/jp304068a

[39] Vaari, J., J. Lahtinen, and P. Hautojärvi. "The adsorption and decomposition of acetylene on clean and K-covered Co (0001)." *Catalysis letters* 44, no. 1 (1997): 43-49. https://doi.org/10.1023/A:1018972924563

[40] Kim, Eunho, Hyosub An, Hyunchul Jang, Won-Ju Cho, Naesung Lee, Wan-Gyu Lee, and Jongwan Jung. "Growth of Few-Layer Graphene on a Thin Cobalt Film on a Si/SiO2 Substrate." *Chemical Vapor Deposition* 17, no. 1-3 (2011): 9-14. https://doi.org/10.1002/cvde.201004296

[41] Sutter, Peter, Jerzy T. Sadowski, and Eli Sutter. "Graphene on Pt (111): Growth and substrate interaction." *Physical Review B—Condensed Matter and Materials Physics* 80, no. 24 (2009): 245411. https://doi.org/10.1103/PhysRevB.80.245411

[42] Coraux, Johann, Martin Engler, Carsten Busse, Dirk Wall, Niemma Buckanie, Frank-J. Meyer Zu Heringdorf, Raoul Van Gastel, Bene Poelsema, and Thomas Michely. "Growth of graphene on Ir (111)." *New Journal of Physics* 11 (2009): 023006. https://doi.org/10.1088/1367-2630/11/2/023006

[43] Shinde, Dhanraj B., Pavan Chaturvedi, Ivan V. Vlassiouk, and Sergei N. Smirnov. "Unique role of dimeric carbon precursors in graphene growth by chemical vapor deposition." *Carbon Trends* 5 (2021): 100093. https://doi.org/10.1016/j.cartre.2021.100093

[44] Zietz, Otto, Samuel Olson, Brendan Coyne, Yilian Liu, and Jun Jiao. "Characterization and manipulation of carbon precursor species during plasma enhanced chemical vapor deposition of graphene." *Nanomaterials* 10, no. 11 (2020): 2235. https://doi.org/10.3390/nano10112235

[45] Kondrashov, Ivan, Maxim Komlenok, Pavel Pivovarov, Sergey Savin, Elena Obraztsova, and Maxim Rybin. "Preparation of copper surface for the synthesis of single-layer graphene." *Nanomaterials* 11, no. 5 (2021): 1071. https://doi.org/10.3390/nano11051071

[46] Kostogrud, I. A., E. V. Boyko, and D. V. Smovzh. "Effect of hydrogen concentration on CVD synthesis of graphene." In *Journal of Physics: Conference Series*, vol. 1382, no. 1, p. 012157. IOP Publishing, 2019. https://doi.org/10.1088/1742-6596/1382/1/012157

[47] Nalini, Savitha, Subin Thomas, M. K. Jayaraj, and K. Rajeev Kumar. "Analysis of graphene films grown on copper foil at 845° C by intermediate pressure chemical vapor deposition." *Materials Research Express* 5, no. 11 (2018): 115604. https://doi.org/10.1088/2053-1591/aadec4

[48] Eversteyn, F. C., P. J. W. Severin, C. H. J. vd Brekel, and H. L. Peek. "A stagnant layer model for the epitaxial growth of silicon from silane in a horizontal reactor." *Journal of The Electrochemical Society* 117, no. 7 (1970): 925. https://doi.org/10.1149/1.2407685

[49] Kleijn, C. R., Th H. Van Der Meer, and C. J. Hoogendoorn. "A mathematical model for LPCVD in a single wafer reactor." *Journal of The Electrochemical Society* 136, no. 11 (1989): 3423. https://doi.org/10.1149/1.2096465

[50] Kleijn, C. R. "A mathematical model of the hydrodynamics and gas-phase reactions in silicon LPCVD in a single-wafer reactor." *Journal of the Electrochemical Society* 138, no. 7 (1991): 2190. https://doi.org/10.1149/1.2085948

[51] Visser, E. P., C. R. Kleijn, C. A. M. Govers, C. J. Hoogendoorn, and L. J. Giling. "Return flows in horizontal MOCVD reactors studied with the use of TiO2 particle injection and numerical calculations." *Journal of Crystal Growth* 94, no. 4 (1989): 929-946. https://doi.org/10.1016/0022-0248(89)90127-9

[52] Giling, L. J. "Temperatures and flows in horizontal epi reactors." *Le Journal de Physique Colloques* 43, no. C5 (1982): C5-235. https://doi.org/10.1051/jphyscol:1982528

[53] Giling, L. J. "Gas flow patterns in horizontal epitaxial reactor cells observed by interference holography." *Journal of The Electrochemical Society* 129, no. 3 (1982): 634. https://doi.org/10.1149/1.2123939

[54] Coltrin, Michael E., Robert J. Kee, and James A. Miller. "A mathematical model of the coupled fluid mechanics and chemical kinetics in a chemical vapor deposition reactor." *Journal of the Electrochemical Society* 131, no. 2 (1984): 425. https://doi.org/10.1149/1.2115598

[55] Fauzi, Fatin Bazilah, Edhuan Ismail, Syed Noh Syed Abu Bakar, Ahmad Faris Ismail, Mohd Ambri Mohamed, Muhamad Faiz Md Din, Suhaimi Illias, and Mohd Hanafi Ani. "The role of gas-phase dynamics in interfacial phenomena during few-layer graphene growth through atmospheric pressure chemical vapour deposition." *Physical Chemistry Chemical Physics* 22, no. 6 (2020): 3481-3489. https://doi.org/10.1039/C9CP05346H

[56] Li, Gan, Sheng-Hong Huang, and Zhenyu Li. "Gas-phase dynamics in graphene growth by chemical vapour deposition." *Physical Chemistry Chemical Physics* 17, no. 35 (2015): 22832-22836. https://doi.org/10.1039/C5CP02301G

[57] Osman, Muhammad Naqib, Mohd Hanafi Ani, and Syed Noh Syed Abu Bakar. "Substrate Placement inside CVD Tube for Graphene Production." In *Materials Science Forum*, vol. 981, pp. 84-91. Trans Tech Publications Ltd, 2020. https://doi.org/10.4028/www.scientific.net/MSF.981.84

[58] Bulsari, Abhay B., Mark E. Orazem, and James G. Rice. "The influence of axial diffusion on convective heat and mass transfer in a horizontal CVD reactor." *Journal of crystal growth* 92, no. 1-2 (1988): 294-310. https://doi.org/10.1016/0022-0248(88)90462-9

[59] Fotiadis, Dimitrios I., Martin Boekholt, Klavs F. Jensen, and Wolfgang Richter. "Flow and heat transfer in CVD reactors: comparison of Raman temperature measurements and finite element model predictions." *Journal of crystal growth* 100, no. 3 (1990): 577-599. https://doi.org/10.1016/0022-0248(90)90257-L
[60] Khanafer, K., and M. F. Lightstone. "Computational modeling of transport phenomena in chemical vapor deposition." *Heat and mass transfer* 41 (2005): 483-494. https://doi.org/10.1007/s00231-004-0571-z
[61] Cheng, T. S., and M. C. Hsiao. "Numerical investigations of geometric effects on flow and thermal fields in a horizontal CVD reactor." *Journal of crystal growth* 310, no. 12 (2008): 3097-3106. https://doi.org/10.1016/j.jcrysgro.2008.03.007
[62] Zhang, Pan, Wang Weiwen, Guanghui Cheng, and Li Jianlong. "Effect of boundary layers on polycrystalline silicon chemical vapor deposition in a trichlorosilane and hydrogen system." *Chinese Journal of Chemical Engineering* 19, no. 1 (2011): 1-9. https://doi.org/10.1016/S1004-9541(09)60169-5
[63] Bhaviripudi, Sreekar, Xiaoting Jia, Mildred S. Dresselhaus, and Jing Kong. "Role of kinetic factors in chemical vapor deposition synthesis of uniform large area graphene using copper catalyst." *Nano letters* 10, no. 10 (2010): 4128-4133. https://doi.org/10.1021/nl102355e
[64] Łach, Łukasz, and Dmytro Svyetlichnyy. "Recent Progress in Heat and Mass Transfer Modeling for Chemical Vapor Deposition Processes." *Energies* 17, no. 13 (2024): 3267. https://doi.org/10.3390/en17133267
[65] Bokobza, Liliane, Jean-Luc Bruneel, and Michel Couzi. "Raman spectroscopy as a tool for the analysis of carbon-based materials (highly oriented pyrolitic graphite, multilayer graphene and multiwall carbon nanotubes) and of some of their elastomeric composites." *Vibrational Spectroscopy* 74 (2014): 57-63. https://doi.org/10.1016/j.vibspec.2014.07.009
[66] McComas, S. T., and Ernst Rudolf Georg Eckert. "Combined free and forced convection in a horizontal circular tube." (1966): 147-152. https://doi.org/10.1115/1.3691494
[67] Chatterjee, Shahana, Thomas Abadie, Meihui Wang, Omar K. Matar, and Rodney S. Ruoff. "Repeatability and Reproducibility in the Chemical Vapor Deposition of 2D Films: A Physics-Driven Exploration of the Reactor Black Box." *Chemistry of Materials* 36, no. 3 (2024): 1290-1298. https://doi.org/10.1021/acs.chemmater.3c02361
[68] Li, Zhancheng, Wenhua Zhang, Xiaodong Fan, Ping Wu, Changgan Zeng, Zhenyu Li, Xiaofang Zhai, Jinlong Yang, and Jianguo Hou. "Graphene thickness control via gas-phase dynamics in chemical vapor deposition." *The Journal of Physical Chemistry C* 116, no. 19 (2012): 10557-10562. https://doi.org/10.1021/jp210814j
[69] Yang, Bo, Ni Yang, Dan Zhao, Fengyang Chen, Xingping Yuan, Yanqing Hou, and Gang Xie. "Numerical Simulation of a Simplified Reaction Model for the Growth of Graphene via Chemical Vapor Deposition in Vertical Rotating Disk Reactor." *Coatings* 13, no. 7 (2023): 1184. https://doi.org/10.3390/coatings13071184
[70] Mizuno, Yoshichika, and Shin-ichiro Uekusa. "Analysis of reaction gases flow in CVD processes." *Materials Science and Engineering: B* 35, no. 1-3 (1995): 156-159. https://doi.org/10.1016/0921-5107(95)01358-X
[71] Johari, Muhammad Hilmi, Mohamad Shukri Sirat, Mohd Ambri Mohamed, Ahmad Fikri Mustaffa, and Abdul Rahman Mohmad. "Computational Fluid Dynamics Insights into Chemical Vapor Deposition of Homogeneous MoS2 Film with Solid Precursors." *Crystal Research and Technology* 58, no. 10 (2023): 2300139. https://doi.org/10.1002/crat.202300139
[72] Mizuno, Yoshichika, and Shin-ichiro Uekusa. "Hydrodynamic model of thin film deposition." *Microelectronic engineering* 43 (1998): 519-526. https://doi.org/10.1016/S0167-9317(98)00213-5
[73] Wang, Dong, Junyan Lao, Wenjia Xiao, Hengxu Qu, Jie Wang, Gang Wang, and Jian Li. "Theoretical adjustment of metalorganic chemical vapor deposition process parameters for high-quality gallium nitride epitaxial films." *Physics of Fluids* 35, no. 3 (2023). https://doi.org/10.1063/5.0141060
[74] Mizuno, Yoshichika, Shin-ichiro Uekusa, and Hideyuki Okabe. "Hydrodynamic description of epitaxial film growth in a horizontal reactor." *Journal of crystal growth* 170, no. 1-4 (1997): 61-65. https://doi.org/10.1016/S0022-0248(96)00566-0
[75] Tian, Jing, Zhuorui Tang, Hongyu Tang, Jiajie Fan, and Guoqi Zhng. "Optimizing Temperature and Flow Fields of 4H-SiC Epitaxial Growth by Integrating CFD Simulation with Multi-objective Particle Swarm Optimization." In *2023 24th International Conference on Electronic Packaging Technology (ICEPT)*, pp. 1-7. IEEE, 2023. https://doi.org/10.1109/ICEPT59018.2023.10492175
[76] Stock, L., and W. Richter. "Vertical versus horizontal reactor: An optical study of the gas phase in a MOCVD reactor." *Journal of Crystal Growth* 77, no. 1-3 (1986): 144-150. https://doi.org/10.1016/0022-0248(86)90294-0
[77] Li, Lei, Muhammad Thalhah Zainal, Mohd Fairus Mohd Yasin, Norikhwan Hamzah, Mohsin Mohd Sies, Muhammad Noor Afiq Witri Muhammad Yazid, Shokri Amzin, and Aizuddin Supee. "The influences of oxygen concentration and external heating on carbon nanotube growth in diffusion flame." *CFD Letters* 13, no. 12 (2021): 45-62. https://doi.org/10.37934/cfdl.13.12.4562